

NOVEL TRIANGULAR METAMATERIAL DESIGN FOR ELECTROMAGNETIC ABSORPTION REDUCTION IN HUMAN HEAD

Mohammad R. I. Faruque* and **Mohammad T. Islam**

Institute of Space Science (ANGKASA), Faculty of Engineering and Built Environment, Universiti Kebangsaan Malaysia, UKM, Bangi, Selangor 43600, Malaysia

Abstract—In this paper, a novel triangular metamaterial (TMM) structure, which exhibits a resonating electric response at microwave frequency, is developed by etching two concentric triangular rings of conducting materials. A finite-difference time-domain method in conjunction with the lossy-Drude model was used in this study. Simulations were performed using the CST Microwave Studio®. The technique of specific absorption rate (SAR) reduction is discussed, and the effects of the position of attachment, the distance, and the size of the metamaterials on the SAR reduction are explored. The performance of the novel TMMs in cellular phones was also measured in the cheek and the tilted positions using the COMOSAR system. The TMMs achieved a 50.82% reduction for 1 gm SAR. These results provide a guideline to determine the triangular design of metamaterials with the maximum SAR reducing effect for a cellular phone.

1. INTRODUCTION

The possible health risk caused by mobile communication handsets due to their electromagnetic (EM) interaction with user's head and the means of protecting against the impact of this interaction are global concerns. There is a significant need to evaluate electromagnetic absorption by the human head during the uses of electronic devices such as mobile phones. The user's body, especially head and hand, affects the voltage standing-wave ratio (VSWR) and gain of the antenna, as well as the radiation pattern produced by the antenna. Furthermore, thermal effects, particularly when tissues are exposed to unlimited amounts of electromagnetic energy, can be a serious

Received 6 May 2013, Accepted 6 July 2013, Scheduled 29 July 2013

* Corresponding author: Mohammad Rashed Iqbal Faruque (rashedgen@yahoo.com).

health hazard. To address the potential health hazards, standards organizations have set exposure limits known as the specific absorption rate (SAR) [1–10]. Simplified phone antennas, such as half-wavelength dipoles in free space or quarter-wavelength monopoles mounted onto a metallic box, have been frequently investigated in the literature [11–16]. These types of antennas are no longer in widespread use for cellular phones and therefore are not suitable for studying the interaction of handset antennas and nearby tissues.

The main breakthrough of metamaterials is their ability to efficiently guide and control electromagnetic waves through the engineering of their material structure. In recent years, significant research has been performed worldwide with the purpose to study, develop and design metamaterials and their applications, particularly in electromagnetics [17–22]. Metamaterials are artificially fabricated structures that have new, physically realizable response functions that do not occur or may not be readily available in nature. Electric permittivity and magnetic permeability are the two important parameters because they determine how the metamaterials respond in electromagnetic fields. For example, a negative permittivity can be achieved by placing the thin metallic wires sporadically [23] or with an array of split ring resonators (SRRs). The use of a SRRs-design operating at 1.8 GHz was used to reduce the SAR value in a lossy material as discussed in Refs. [24–26]. The metamaterials based on SRRs are designed on a printed circuit board, which enables simple integration into cellular phones. The authors used the FDTD method with lossy-Drude models to simulate the metamaterials. This simulation method is useful to study the wave propagation characteristics of metamaterials [27–30]. The method has been updated using the perfectly matched layer (PML), thus extending the simulation capability to three-dimensional problems.

In this paper, we focus on artificial structures to design double negative TMMs that are attached onto the PCB of mobile phones to reduce the SAR in the human head. This paper is structured as follows. Section 2 describes the numerical analysis of the handset in conjunction with the SAM phantom head. The FDTD method is used with positive meshing techniques for quick and correct analyses. The modeling and analyzing FDTD method with lossy-Drude model for SAR reduction are also discussed in Section 2. The impacts on SAR of the attachment of metamaterials are analyzed in Section 3. The new design of a triangular split ring resonators (TSRRs) structure, the design simulation, and the fabrication of metamaterials are explained in Section 4. Section 5 describes the experimental validation of the measurement results, and Section 6 concludes the paper.

2. METHODOLOGY

2.1. Model Description

The simulation model, which includes the handset with the PIFA-type of antenna and the SAM phantom head provided by CST Microwave Studio[®] (CST MWS), was used in this study. An inclusive handset model, consisting of the circuit board, LCD display, keypad, battery and housing, was used in the numerical calculation. The relative permittivity and conductivity of the individual components were set to comply with industrial standards. In addition, the definitions in [3] were adopted for the material parameters involved in the SAM phantom head. To precisely characterize the performance over a broad frequency range, dispersive models for all the dielectrics were used in the simulation [11, 12].

The electrical properties of the materials used for simulation are listed in Table 1. In the simulation model, a helical PIFA-type antenna was used, which is used for GSM 900 MHz applications. A high-quality geometrical approximation can be obtained for such a structure by using the meshing scheme of FDTD method. The use of this meshing scheme in turn led to challenges in obtaining convergent results within a short simulation time.

Table 1. Electrical properties of the materials considered in the simulation.

Phone Materials	ϵ_r	σ (S/m)
Circuit Board	4.4	0.05
Housing Plastic	2.5	0.005
LCD Display	3.0	0.02
Rubber	2.5	0.005
SAM Phantom Head		
Shell	3.7	0.0016
Liquid @ 900 MHz	40	1.42

2.2. Numerical Method

The SAR reduction using metamaterials was studied by determining the EM fields in a specified tissue domain using a three-dimensional FDTD method, which was implemented in commercial software from Computer Simulation Technology (CST MWS). A non-uniform meshing scheme was adopted to enable the major computational power to be dedicated to the regions along the inhomogeneous boundaries

for rapid and flawless analysis. The minimum and maximum mesh sizes were 0.3 mm and 1.0 mm, respectively. The complete model was reduced to a total of 2,097,152 mesh cells. The simulation time was 1163 s (including mesh generation) for each run on a computer system based on an Intel Core™ 2 Duo E 8400 3.0 GHz CPU with 4 GB of RAM.

The analysis workflow used in the work described in this paper began with the design of the antenna to be studied in an inclusive handset model in free space (i.e., without absorbing tissue). The antenna was designed such that the S_{11} response was less than -10 dB over the frequency band of interest. The SAM phantom human head was then included for SAR calculation using the standard definition [29]:

$$\text{SAR} = \frac{\sigma}{2\rho} E^2. \quad (1)$$

where E is the induced electric field (V/m), ρ is the tissue density (kg/m^3), and σ is the tissue conductivity (S/m). The resultant SAR values averaged over 1 gm and 10 gm of tissue in the head were denoted as SAR 1 gm and SAR 10 gm, respectively. These SAR values were used as a benchmark to appraise the effectiveness in the peak SAR reduction.

The effectiveness of the SAR reduction and the antenna performance in different arrangements, sizes, and material properties of the materials and the metamaterials determined from the simulations will be presented. The head models used in this study were based on a MRI-based head model from the website named “whole brain Atlas”. Six types of tissues, bone, brain, muscle, eye ball, fat, and skin were used in this model [28]. Numerical simulations of the SAR value were performed using the FDTD method. The parameters for the FDTD computation were as follows. The simulation domain was $128 \times 128 \times 128$ cells. The cell sizes were set as $\Delta x = \Delta y = \Delta z = 1$ mm. The computational domain was terminated with 8 cells of a perfect matched layer (PML). A PIFA antenna was modeled using the thin-wire approximation.

Figure 1 shows a handset with the antenna at 900 MHz considered in this study. This handset was modeled as a quarter-wavelength PIFA antenna positioned onto a rectangular conducting box with dimensions of 10 cm height, 4 cm width, and 3 cm thickness. The PIFA antenna was placed on the top surface of the conducting box. The SAM head model used in this research consisted of approximately 2,097,152 cubical cells of 1 mm resolution. A time-step of 0.1 nanoseconds was used in the simulation, and the simulation duration was approximately eight sinusoidal cycles to ensure steady state conditions. The second-

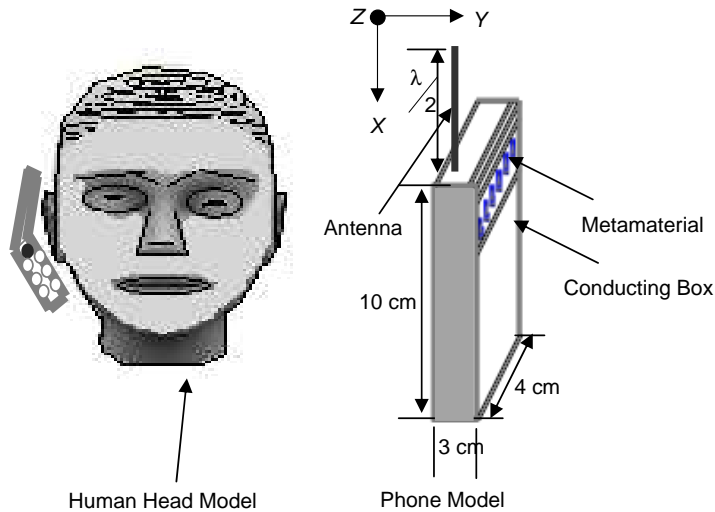


Figure 1. The head and phone models used in the SAR calculations.

order Mur absorbing boundaries acting on the electric fields were implemented to absorb the outgoing scattered waves. An antenna excitation was introduced by specifying a sinusoidal voltage diagonally at the one-cell gap between the helix and the top surface of the conducting box.

3. IMPACT OF THE METAMATERIAL ATTACHMENT ON THE SAR

In this section, the designed TSRs were placed in between a human head and the antenna. This arrangement reduced the SAR value. To study this reduction at the GSM 900 band, different positions, sizes, and metamaterials were also analyzed by using the FDTD method to implement the detailed human head model.

The dispersive models for all the dielectrics were used for the simulation to accurately analyze the TSRs. The antenna was aligned to be parallel to the head axis. The distance between the antenna and the head was varied from 5 mm to 20 mm. Finally, a distance of 20 mm was chosen to perform the comparison between the different metamaterials. The output power of the mobile phone model was set before the SAR was simulated. In this paper, the output power of the cellular phone was set to 600 mW at the operating frequency of 900 MHz. In the real world, the output power of the mobile phone

will not exceed 250 mW for normal use, while the maximum output power can reach to 1 W or 2 W when the base station is far away from the mobile station (cellular phone). The SAR simulation results were compared with the results in [1, 11], and [28] for validation. When the phone model was placed 20 mm away from the human head model without a metamaterial, the simulated SAR 1 gm peak value was 2.002 W/kg, and the SAR 10 gm value was 1.293 W/kg. The level of SAR reduction is higher with metamaterial attachments. The result reported in [1] and [11] are 2.17 W/kg and 2.28 W/kg, respectively, for the SAR 1 gm value. These respective reported SAR levels are due to the mobile antenna position, i.e., the antenna structures were not properly aligned and antennae themselves were also different. These SAR values are significantly better than the result reported in [28], which was 2.43 W/kg for the SAR 1 gm value. This reported SAR value was achieved via different radiating powers and antenna designs.

The distance from the antenna feeding point to the edge of the metamaterial was $A = 3$ mm. The size of the metamaterial in the x - z plane was 62 mm \times 38 mm, and the thickness was 6 mm. The SAR value and the antenna performance with the metamaterial were studied. To calculate the antenna's radiated power, the source impedance (Z_S) was assumed to be the complex conjugate of the free space radiation impedance ($Z_S = 105.18 + j81.97 \Omega$). The source voltage (V_S) was chosen so that the radiated power in free space is equal to 600 mW ($V_S = \sqrt{0.6 \cdot 8 \cdot R_{R0}}$). The source impedance and source voltage were held constant at the Z_S and V_S values when analyzing the effect of the metamaterials and the human head on the antenna performance.

The power radiated from the antenna was calculated by comparing the radiation impedance in this situation ($Z_R = R_R + jX_R$) with that using the following [30] equation:

$$P_R = \frac{1}{2} V_S^2 \frac{R_R}{|Z_R + Z_S|^2}. \quad (2)$$

The total power absorbed in the head was calculated by

$$P_{abs} = \frac{1}{2} \int_V \sigma |E|^2 dv. \quad (3)$$

Different negative medium parameters were investigated to study the efficiency of the SAR reduction effectiveness. We positioned the negative permittivity media between the antenna and the human head to intercept the electromagnetic waves. Initially, the plasma frequencies of the media were set to be $\omega_{pe} = 9.239 \times 10^9$ rad/s, which resulted in media with $\mu = 1$ and $\varepsilon = -3$ at 900 MHz. The media with larger negative permittivity $\mu = 1$, and $\varepsilon = -5$; $\mu = 1$, and $\varepsilon = -7$ were also analyzed. We set $\Gamma_e = 1.22 \times 10^8$ rad/s, indicating

that the media have losses. The SAR 1 gm peak level reduces to 1.0724 W/kg with $\mu = 1$ and $\varepsilon = -3$ media, and the impedance is affected by metamaterials as well. Compared to the control experiment without metamaterials, the radiated power was reduced by 14.55%, while the SAR was reduced by 46.44%. When traditional media are used, the SAR reduction effectiveness is decreased compared to that of the metamaterials. In addition, the radiated power from the antenna is nearly unaffected when the metamaterials were used. Comparisons of the SAR reduction effectiveness with different positions and sizes of the metamaterials were performed.

The radiation patterns of the PIFA antenna combined with $\mu = 1$ and $\varepsilon = -3$ metamaterials were analyzed to further examine whether the metamaterials affect the antenna performance. The radiation patterns were obtained by the near- and far-field transformation of the Kirchhoff surface integral representation (KSIR) [18]. All the radiation patterns were normalized to the maximum gain attained without any added materials. Figure 2 shows the radiation patterns in the φ plane for $\theta = 90^\circ$. In [3], the radiation pattern close to the head is reduced by approximately 6 dB, which agrees with our simulation results. With the use of metamaterials, the maximum degradation of the far field was observed to not exceed 1.22 dB. In addition, even in every other antenna orientation, the mobile phone power does not change significantly.

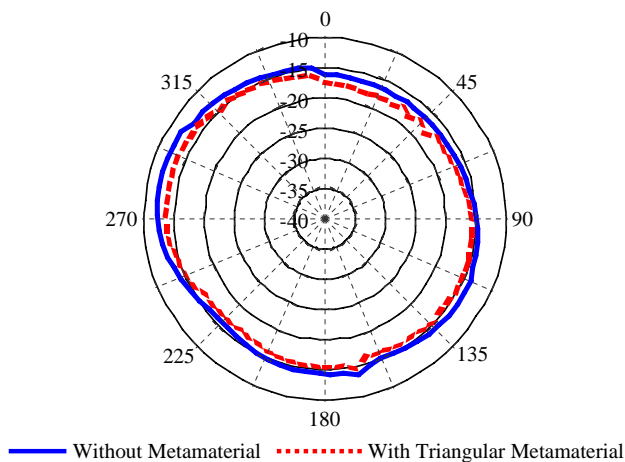


Figure 2. Calculated \varnothing plane radiation pattern at 900 MHz.

4. METHODOLOGY AND ANALYSIS OF SAR FOR THE PROPOSED TSRRs

The SAR in the head is reduced by placing the triangular metamaterials (TMMs) between the antenna and the head. Note that the TMMs are smaller than the operating wavelength and that the structures resonate due to their internal capacitance and inductance. The stop band can be tuned to the operational bands of cellular phone radiation. The TMMs were designed on a printed circuit board to allow them to be easily integrated into cellular phones. The overall dimensions of the TMMs were determined by periodic arrangement of the sub-wavelength resonators.

4.1. Construction and Design of the TSRRs

This research establishes that using FDTD analysis, TMMs can reduce the SAR 1 gm and SAR 10 gm peak levels in the head. In this section, the TMMs are evaluated in the cellular phone 900 and 1800 MHz bands. Periodically arranged TSRRs can work as TMMs. The TSRRs structure consists of two concentric triangular rings. Both triangular rings have a gap, and each ring is placed opposite to the gap of the other ring. The schematic of the TSRRs structure used in this study is shown in Figure 3.

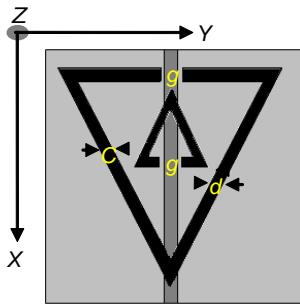


Figure 3. The structure of the TSRRs.

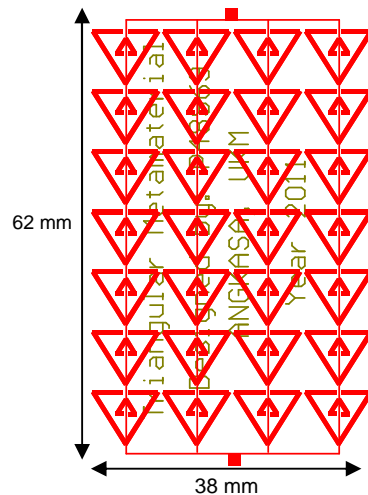


Figure 4. Arrays of TSRRs.

To construct the TMMs for SAR reduction, the TSRRs were used as the resonator model, as shown in Figure 3. The resonators operated in the 900 MHz band. The TSRRs consist of two triangular rings, each with gaps on the opposite sides [2]. Note that the SRRs were introduced by Pendry et al. (1999) [29], and subsequently used by Smith et al. (2000) to synthesize the first left-handed artificial medium [31]. The metamaterials in this work were designed with periodic TSRRs arrangements to reduce the SAR value. By properly designing the TSRRs structure parameters, a negative effective medium parameter can be achieved for both the 900 and 1800 MHz bands.

In Figure 3, the resonator structures are defined by the following structure parameters: the triangular ring thickness c , triangular ring gap d , triangular ring size l , and split gap g . Here, c_0 is the speed of light in free space and r the radius of the inner ring.

Figure 4 presents the TSRRs arrays used for the SAR calculations in this work. These arrays were divided into four columns and seven rows. The TSRRs arrays considered in this work were of dimensions $62 \text{ mm} \times 38 \text{ mm}$.

4.2. Results and Discussion

Numerical simulations that predict the transmission properties are dependent on the system's various structure parameters. Simulations of such complexity are typically performed by the FDTD method. Periodic boundary conditions can reduce the computational domain, while an absorbing boundary condition can be used to represent the propagation regions. The total-field/scatter-field formulation excites the plane wave. The regions inside the computational domain and those outside the TSRRs were set to be vacuums.

To verify our FDTD simulation, the structure parameters of the TSRRs were set to those of [13]: $d = g = c = 0.33 \text{ mm}$ and $l = 3 \text{ mm}$. The thickness and dielectric constant of the circuit board were 4.4 mm and 0.45 , respectively. Twenty-eight unit elements were used in the propagation direction. Periodic boundary conditions were implemented normal to the direction of propagation. Figure 5 illustrates the simulated and measured transmission spectra of the TSRRs studied. In [27], the measured results indicate that the SRRs exhibit a stop band extending from 8.1 to 9.5 GHz , whereas in this work, the simulation and the measured results indicate that the TSRRs exhibit a stop band extending from 8.3 to 9.4 GHz . This difference is due to the use of the square ring SRRs in [27] and the modified TSRRs with novel TMMs shape used in this research.

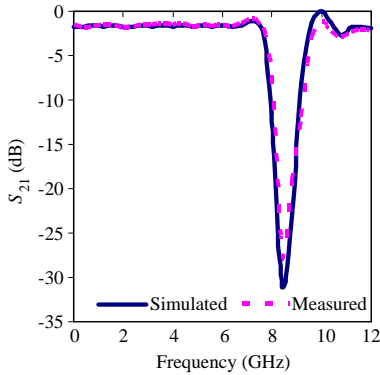


Figure 5. Modeled transmission spectra of the TSRRs plane in the yz plane.

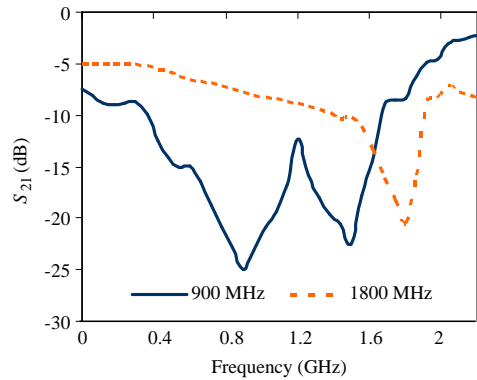


Figure 6. Modeled transmission spectra of the designed TSRRs.

The stop bands of the TSRRs were designed to be at 900 MHz and 1800 MHz. The periodicity along the x -, y -, and z -axes were $L_x = 62$ mm, $L_y = 1.5$ mm, and $L_z = 62$ mm, respectively. To obtain a stop band at 1800 MHz, the TSRRs parameters are chosen to be $c = 1.8$ mm, $d = 0.6$ mm, $g = 0.6$ mm, and $r = 12.7$ mm. The periodicity along the x -, y -, and z -axes were $L_x = 50$ mm, $L_y = 1.5$ mm, and $L_z = 50$ mm, respectively. The thickness and dielectric constant of the circuit boards for both the 900 MHz and 1800 MHz bands were 0.508 mm and 3.38, respectively. Once the geometric parameters were properly chosen, the TSRRs medium can exhibit a stop band at approximately 900 MHz and 1800 MHz.

Note that the size of the designed TSRRs can also be reduced with the use of a high-dielectric-constant circuit board. As shown in Figure 6, the TSRRs medium can exhibit a stop band at 900 and 1800 MHz using properly designed structure parameters. A simple frequency selective surface (FSS) can also be used to obtain a stop band. In [11, 31–34], a number of FSS are proposed for antenna applications. In [4], the authors proposed a CLL structure that is similar to the TSRRs for antenna applications. However, these structures display a stop band at several GHz.

5. EXPERIMENTAL VALIDATION

The SAR measurement was performed using the COMOSAR measurement system. The system uses a robot to position the SAR probe inside the head phantom. The head phantom is filled with a

Table 2. SAR simulation and measurement results without the inclusion of TMMs (distance in between the head & phone model, $d = 20$ mm).

	Value of SAR	
	SAR 1 gm	SAR 10 gm
Simulated	2.002	1.673
Measured	1.936	1.609

liquid with dielectric properties selected based on IEEE standard 1528, which are $\epsilon_r = 41.5$ and $\sigma = 0.97$ S/m for 900 MHz and $\epsilon_r = 40$ and $\sigma = 1.4$ S/m for 1800 MHz. The measured and simulated SAR values without the inclusion of TMMs are listed in Table 2.

Table 2 indicates that the simulated SAR value is greater than 3.29% for the SAR 1 gm value and 3.82% for the SAR 10 gm value, which is because the distance between the head and phone model has not been correctly situated for the measurement stage. In addition, the distance between the source and the internal surface of the phantom position affects the SAR. For a 5 mm distance, a positioning uncertainty of ± 0.5 mm would produce a SAR uncertainty of $\pm 20\%$. Therefore, accurate device positioning is essential for accurate SAR measurements.

Figure 7 presents photographs of the SAR measurement system in the tilted positions. The antennas with the TMMs are in contact with the SAM phantom head. During the measurement, the radiation power has been set to the maximum for the phone being tested (as required by the standard) of 33 dBm for GSM 900.

Figures 8 and 9 show the simulated & measured SAR values obtained using the tilted position for the TMMs with the antenna, which resulted in the simulated and measured SAR 1 gm values of 1.0963 W/kg and 1.017 W/kg, respectively, using the antenna with TMMs.

The simulated and measured SAR values differed by 7.23% for the SAR 1 gm value. Regarding the difference in the absolute values of peak SAR, the phone model casing for the simulation was different from the case used for the measurement. In addition, Scotch tape was used to attach the TMMs and the antenna during the measurement stages. The simulated and measured results also differ because the parameters for the measurement system change with water evaporation and temperature. Furthermore, the measurement system contains several parameters (e.g., source, network emulator, probe, and electronic evaluation procedures) that affect the SAR calculation but are not included in the simulation.



Figure 7. Photograph of the real measurement system for the antenna with the TMMs in the tilted position.

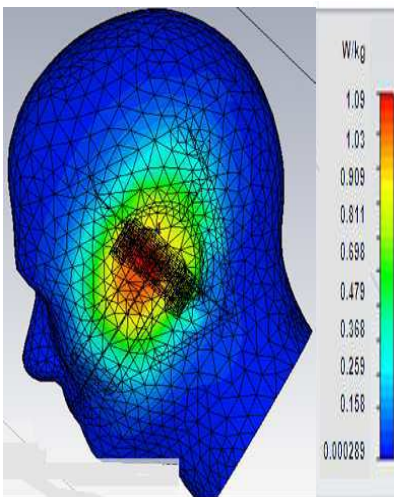


Figure 8. Simulated SAR value of the antenna with TMMs attachment in the tilted position.

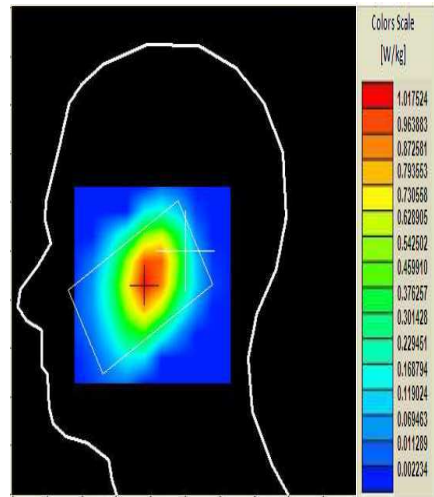


Figure 9. Measured SAR value of the antenna with the TMMs attachment in the tilted position.

6. CONCLUSION

The electromagnetic energy absorption between an antenna and a human head using novel double-negative TMMs was discussed in this paper. Utilizing the proposed metamaterial in the phone model, a SAR value of approximately 0.617 W/kg was achieved for the SAR 10 gm value, and a value of 1.0175 W/kg was achieved for the SAR 1 gm value. Based on the 3-D FDTD method with the lossy-Drude model, both the SAR 1 gm and SAR 10 gm peak values of the head can be reduced by placing metamaterials between the antenna and the human head. The use of all dielectric metamaterials tuned to the exact ϵ and μ values required to divert the electromagnetic energy from the cellular phone user's head are promising options to improve the SAR reductions. Our results provide constructive information for the design of communication equipment that complies with the safety requirements.

REFERENCES

1. Wang, J. and O. Fujiwara, "FDTD computation of temperature rise in the human head for portable telephones," *IEEE Trans. Microwave Theory Tech.*, Vol. 47, No. 8, 1528–1534, Aug. 1999.
2. Faruque, M. R. I., M. T. Islam, and N. Misran, "Design analysis of new metamaterial for EM absorption reduction," *Progress In Electromagnetics Research*, Vol. 124, 119–135, 2012.
3. Manapati, M. B. and R. S. Kshetrimayum, "SAR reduction in human head from mobile phone radiation using single negative metamaterials," *Journal of Electromagnetic Waves and Applications*, Vol. 23, No. 10, 1385–1395, 2009.
4. Kusuma, A. H., A.-F. Sheta, I. M. Elshafiey, Z. Siddiqui, M. A. S. Alkanhal, S. Aldosari, S. A. Alshebeili, and S. F. Mahmoud, "A new low SAR antenna structure for wireless handset applications," *Progress In Electromagnetics Research*, Vol. 112, 23–40, 2011.
5. Zhang, M. and A. Alden, "Calculation of whole-body SAR from a 100 MHz dipole antenna," *Progress In Electromagnetics Research*, Vol. 119, 133–153, 2011.
6. Golestanirad, L., A. P. Izquierdo, S. J. Graham, J. R. Mosig, and C. Pollo, "Effect of realistic modeling of deep brain stimulation on the prediction of volume of activated tissue," *Progress In Electromagnetics Research*, Vol. 126, 1–16, 2012.
7. Islam, M. T., H. Z. Abidin, M. R. I. Faruque, and N. Misran,

- “Analysis of materials effects on radio frequency electromagnetic fields in human head,” *Progress In Electromagnetics Research*, Vol. 128, 121–136, 2012.
8. Ronald, S. H., M. F. B. A. Malek, S. H. Idris, E. M. Cheng, M. H. Mat, M. S. Zulkefli, and S. F. Binti Maharimi, “Designing Asian-sized hand model for SAR determination at GSM900/1800: Simulation part,” *Progress In Electromagnetics Research*, Vol. 129, 439–467, 2012.
 9. Ikeuchi, R., K. H. Chan, and A. Hirata, “SAR and radiation characteristics of a dipole antenna above different finite EBG substrates in the presence of a realistic head model in the 3.5 GHz band,” *Progress In Electromagnetics Research B*, Vol. 44, 53–70, 2012.
 10. Husni, N. A., M. T. Islam, M. R. I. Faruque, and N. Misran, “Effects of electromagnetic absorption towards human head due to variation of its dielectric properties at 900, 1800 and 1900 MHz with different antenna substrates,” *Progress In Electromagnetics Research*, Vol. 138, 367–388, 2013.
 11. Kuo, C. M. and C. W. Kuo, “SAR distribution and temperature increase in the human head for mobile communication,” *IEEE-APS Int. Symp. Dig.*, 1025–1028, Columbus, OH, 2003,
 12. Tay, R. Y. S., Q. Balzano, and N. Kuster, “Dipole configuration with strongly improved radiation efficiency for hand-held transceivers,” *IEEE Trans. Antennas Propagat.*, Vol. 46, No. 6, 798–806, Jun. 1998.
 13. Islam, M. T., M. R. I. Faruque, and N. Misran, “Design analysis of ferrite sheet attachment for SAR reduction in human head,” *Progress In Electromagnetics Research*, Vol. 98, 191–205, 2009.
 14. Yanase, K. and A. Hirata, “Effective resistance of grounded humans for whole-body averaged SAR estimation at resonance frequencies,” *Progress In Electromagnetics Research B*, Vol. 35, 15–27, 2011.
 15. Vidal, N., S. Curto, J. M. Lopez-Villegas, J. Sieiro, and F. M. Ramos, “Detuning study of implantable antennas inside the human body,” *Progress In Electromagnetics Research*, Vol. 124, 265–283, 2012.
 16. Zhang, M. and A. Alden, “Calculation of whole-body SAR from a 100 MHz dipole antenna,” *Progress In Electromagnetics Research*, Vol. 119, 133–153, 2011.
 17. Chen, Z., Y.-L. Ban, J.-H. Chen, J. L.-W. Li, and Y.-J. Wu, “Bandwidth enhancement of LTE/WWAN printed mobile phone antenna using slotted ground structure,” *Progress In*

- Electromagnetics Research*, Vol. 129, 469–483, 2012.
18. Sievenpiper, D., “High-impedance electromagnetic surfaces with a forbidden frequency band,” *IEEE Trans. Microwave Theory Tech.*, Vol. 47, 2059–2074, Nov. 1999.
 19. Kuster, N. and Q. Balzano, “Energy absorption mechanism by biological bodies in the near field of dipole antennas above 300 MHz,” *IEEE Trans. Veh. Technol.*, Vol. 41, No. 1, 17–23, 1992.
 20. Jensen, M. A. and Y. Rahmat-Samii, “EM interaction of handset antennas and a human in personal communications,” *Proc. of the IEEE*, Vol. 83, 7–17, 1995.
 21. Okoniewski, M. and M. A. Stuchly, “A study of the handset antenna and human body interaction,” *IEEE Trans. Microwave Theory Tech.*, Vol. 44, 855–1864, 1996.
 22. Caloz, C. and T. Itoh, *Electromagnetic Metamaterials, Transmission Line Theory and Microwave Applications*, John Wiley & Sons, Inc., 2005.
 23. Ziolkowski, R. W., “Design, fabrication, and testing of double negative metamaterials,” *IEEE Trans. Antennas Propagat.*, Vol. 51, No. 7, 1516–1529, Jul. 2003.
 24. Wu, Z., B.-Q. Zeng, and S. Zhong, “A double-layer chiral metamaterial with negative index,” *Journal of Electromagnetic Waves and Applications*, Vol. 24, No. 7, 983–992, 2010.
 25. Petrillo, L., F. Jangal, M. Darces, J.-L. Montmagnon, and M. Helier, “Negative permittivity media able to propagate a surface wave,” *Progress In Electromagnetics Research*, Vol. 115, 1–10, 2011.
 26. Hasar, U. C. and J. J. Barroso, “Retrieval approach for determination of forward and backward wave impedances of bianisotropic metamaterials,” *Progress In Electromagnetics Research*, Vol. 112, 109–124, 2011.
 27. Bayindir, M., K. Aydin, and E. Ozbay, “Transmission properties of composite metamaterials in free space,” *Appl. Phys. Lett.*, Vol. 81, No. 1, 120–122, Jul. 2002.
 28. Hawang, J. N. and F.-C. Chen, “Reduction of the peak SAR in the human head with metamaterials,” *IEEE Trans. Antennas Propagat.*, Vol. 54, No. 12, 3763–3770, Dec. 2006.
 29. Pendry, J. B., A. J. Holen, D. J. Robbins, and W. J. Stewart, “Magnetism from conductors and enhanced nonlinear phenomena,” *IEEE Trans. Microwave Theory Tech.*, Vol. 47, No. 11, 2075–2084, Nov. 1999.
 30. Faruque, M. R. I., M. T. Islam, and N. Misran, “Analysis

- of electromagnetic absorption in the mobile phones using metamaterials,” *Electromagnetics Journal*, Vol. 31, No. 3, 215–232, 2011.
31. Smith, D. R., W. J. Padilla, D. C. Vier, S. C. Nemat-Nasser, and S. Schultz, “Composite medium with simultaneously negative permeability and permittivity,” *Phys. Rev. Lett.*, Vol. 84, No. 18, 4184–4187, 2000.
 32. Sajin, G. I., “Impedance measurement of millimeter wave metamaterial antennas by transmission line stubs,” *Progress In Electromagnetics Research Letters*, Vol. 26, 59–68, 2011.
 33. De la Mata Luque, T. M., N. R. K. Devarapalli, and C. G. Christodoulou, “Investigation of bandwidth enhancement in volumetric left-handed metamaterials using fractals,” *Progress In Electromagnetics Research*, Vol. 131, 185–194, 2012.
 34. Burlak, G., “Spectrum of cherenkov radiation in dispersive metamaterials with negative refraction index,” *Progress In Electromagnetics Research*, Vol. 132, 149–158, 2012.